PHYSICAL REVIEW D **95,** 123001 (2017)

High energy neutrinos from the tidal disruption of stars

Cecilia Lunardini[1,*] and Walter Winter[2,†]

[1]*Department of Physics, Arizona State University, 450 E. Tyler Mall, Tempe, Arizona 85287-1504, USA*
[2]*Deutsches Elektronen-Synchrotron (DESY), Platanenallee 6, D-15738 Zeuthen, Germany*

(Received 3 February 2017; published 2 June 2017)

We study the production of high energy neutrinos in jets from the tidal disruption of stars by supermassive black holes. The diffuse neutrino flux expected from these tidal disruption events (TDEs) is calculated both analytically and numerically, taking into account the dependence of the rate of TDEs on the redshift and black hole mass. We find that ∼10% of the observed diffuse flux at IceCube at an energy of about 1 PeV can come from TDEs if the characteristics of known jetted tidal disruption events are assumed to apply to the whole population of these sources. If, however, plausible scalings of the jet Lorentz factor or variability time scale with the black hole mass are taken into account, the contribution of the lowest mass black holes to the neutrino flux is enhanced. In this case, TDEs can account for most of the neutrino flux detected at IceCube, describing both the neutrino flux normalization and spectral shape with moderate baryonic loadings. While the uncertainties on our assumptions are large, a possible signature of TDEs as the origin of the IceCube signal is the transition of the flux flavor composition from a pion beam to a muon damped source at the highest energies, which will also result in a suppression of Glashow resonance events.

DOI: 10.1103/PhysRevD.95.123001

I. INTRODUCTION

It is an established fact that supermassive black holes (SMBH) inhabit the center of most or all galaxies. The physics of these objects is still mysterious in many ways and can be studied by observing the effects that the enormous gravitational field of a SMBH produces on the surrounding gas and stellar matter.

A particularly dramatic effect is a tidal disruption event (TDE), the phenomenon in which a star passing within a critical distance from the SMBH is torn apart by its extremely strong tidal force. The accretion of the disrupted stellar matter on the SMBH can generate observable flares of radiation in the thermal, UV, and x rays that might last for days, months, or even years [1–4]. These flares have the potential to reveal important information on the innermost stellar population of a galaxy and on the physics of SMBH. TDEs are especially valuable as probes of SMBH that are normally quiet—as opposed to the active galactic nuclei—and therefore more difficult to study. In a recent catalog [5] (see also Ref. [6]), 66 TDE candidates have been identified with various degrees of confidence. Roughly, observations confirm the general theory of tidal disruption, whereas they leave many open questions on the energetics and dynamics of these phenomena—and possible selection biases in their detection; see e.g. Ref. [7].

Interestingly, a subset of all the observed TDEs shows evidence for a relativistic jet and exhibits a significantly higher luminosity in x rays. The best observed jetted TDE is Swift J1644 + 57 [8]; others are Swift J2058.4 + 0516 [9] and Swift J1112.2 − 8238 [10] (the latter being somewhat atypical; see [5]). Other transient events have been proposed to be jetted TDEs [11,12], although their interpretation is less robust. It has also been suggested that jetted TDEs might have been observed in the past in gamma rays, as a new class of ultralong gamma ray bursts [13].

If they indeed generate jets, TDEs are candidate sources of cosmic rays. This was first investigated by Farrar and Gruzinov [14], who showed that TDEs naturally meet all the necessary criteria to accelerate protons to energy $E \sim 10^{20}$ eV, and they might be sufficiently abundant to account for the observed ultrahigh energy cosmic ray flux. The following works [15] discussed this result for TDEs with parameters compatible with the Swift J1644 + 57 event, suggesting that they could explain the recently observed cosmic ray hot spot; see also Ref. [16].

Under the hadronic hypothesis, jetted TDEs are also sources of neutrinos, via proton-photon interactions. A prediction of the neutrino flux from a TDE was first published by Wang *et al.* [17] for parameters motivated by Swift J1644 + 57. The corresponding number of events at the IceCube detector was estimated. A follow-up study [18] (see also [19]) shows that TDEs could be hidden neutrino sources, lacking a photon counterpart due to the jet choking inside an envelope made of the debris of the disrupted star.[1]

The topic of TDEs as neutrino sources is especially timely. Indeed, IceCube has discovered a diffuse flux of high-energy astrophysical neutrinos of dominantly extragalactic origin [20]. So far, no class of objects which could

*cecilia.lunardini@asu.edu
†walter.winter@desy.de

[1]We do not consider this possibility in our work.

power most of this flux has been identified. Specifically, the contributions from active galactic nuclei (AGN) blazars [21] and gamma-ray bursts (GRBs) [22,23] have been strongly constrained by stacking the information from many different gamma-ray sources. Furthermore, optically thin sources with neutrino production via proton-proton interactions are constrained by the related gamma-ray production from π^0 decay and its contribution to the diffuse extragalactic gamma-ray backgrounds. Comparisons with observations have shown that starburst galaxies cannot be the dominant source powering the diffuse neutrino flux [24,25]. This favors a photohadronic origin for the neutrinos, because mechanisms with proton-photon interactions can reproduce the spectral shape and flavor composition of the observed neutrinos [26]. It is plausible that photohadronic sources might be hidden in GeV-TeV gamma rays, because the parameters that cause a high neutrino production efficiency at the same time produce high opacity to gamma rays at the highest energies [27].

To summarize, if one single class of sources dominates the observed high-energy neutrino flux, it likely obeys the following criteria: (i) the neutrino production occurs by photohadronic interactions, (ii) the photon counterpart, if any, is more likely to be found in the KeV-MeV energy bands than in the GeV-TeV bands, and (iii) the sources should be abundant enough in the universe, so that each of them individually is sufficiently weak to evade constraints from neutrino multiplet searches [28–30].

In this work, we study the diffuse flux of neutrinos from TDEs, which may address these three criteria. Specifically, we compute the neutrino production from a single TDE and use the existing information on the TDE demographics to compute the *diffuse* flux of neutrinos from TDEs. Parameters motivated by Swift J1644 + 57 observations will be used, with emphasis on the physical scenarios that could reproduce the observed neutrino signal at IceCube. Signatures of a TDE neutrino flux that could be relevant for future observations will be discussed as well.

The paper is structured as follows. In Sec. II the physics of tidal disruption and the cosmological rate of TDEs are discussed. Section III presents the details of the numerical calculation of the neutrino flux from a single TDE, with results for several illustrative combinations of parameters. In Sec. IV results are given for the diffuse flux expected at Earth from a cosmological population of TDEs. A discussion on the compatibility with the IceCube data, and future prospects, is given in Sec. V.

II. PHYSICS OF TDEs

A. Tidal disruption and jet formation

The basic physics of tidal disruption of star by a SMBH was first discussed in the 1970s and 1980s, in a number of seminal papers [1–4]; see Refs. [31,32] for more recent examples. Here we summarize the main aspects for a star of solar mass and radius, $m = M_\odot \simeq 1.99 \times 10^{33}$ g and $R = R_\odot \simeq 6.96 \times 10^{10}$ cm. Let M be the mass of the SMBH.

As it moves closer to the SMBH, the star can be deformed and ultimately destroyed by tidal forces. This happens when the star reaches a distance close enough to the SMBH so that the force on a mass element (inside the star) due to the self-gravity of the star is comparable to the force produced on the same element by the SMBH. This distance is the tidal radius

$$r_t = \left(\frac{2M}{m}\right)^{1/3} R \simeq 8.8 \times 10^{12}\ \text{cm} \left(\frac{M}{10^6\ M_\odot}\right)^{1/3} \frac{R}{R_\odot} \left(\frac{m}{M_\odot}\right)^{-1/3}, \quad (1)$$

and the orbital period at such a radius is

$$\tau_t = 2\pi \left(\frac{r_t^3}{2MG}\right)^{1/2} \simeq 10^4 \text{s} \left(\frac{R}{R_\odot}\right)^{3/2} \left(\frac{m}{M_\odot}\right)^{-1/2}. \quad (2)$$

It is useful to compare these quantities with the SMBH Schwarzschild radius

$$R_s = \frac{2MG}{c^2} \simeq 3 \times 10^{11}\ \text{cm} \left(\frac{M}{10^6\ M_\odot}\right), \quad (3)$$

and the corresponding time scale

$$\tau_s \sim 2\pi R_s/c \simeq 63\ \text{s} \left(\frac{M}{10^6\ M_\odot}\right). \quad (4)$$

Here τ_s is a good approximation of the orbital period at the innermost stable circular orbit, for a Schwarzschild black hole (in the observer's frame, see e.g. Ref. [33]).

Comparing r_t with R_s shows that the star will be swallowed whole, with no prior disruption, if $M \gtrsim M_{\max} \simeq 10^8\ M_\odot$. Here a more conservative value, $M_{\max} \simeq 10^{7.2}\ M_\odot$ will be used, motivated by Ref. [7]. As will be clear from Sec. IV A, our results for the diffuse neutrino flux depend weakly on $M_{\max}$.

In the case where disruption occurs, the main phenomenology can be described analytically in terms of basic physics arguments [2]. About $\sim 1/2$ of the mass of the disrupted star becomes bound to the SMBH and is ultimately accreted on it. Therefore, an upper limit to the energy emitted in this event is

$$E_{\max} \sim M_\odot c^2/2 \simeq 9 \times 10^{53}\ \text{erg}, \quad (5)$$

assuming that the change in the SMBH's own internal energy is negligible. After a dark interval of $\mathcal{O}(10)$ days—the time scale of infall of the tightest bound debris—rapid accretion of matter on the SMBH begins. In circumstances where the mass infall rate is sufficiently high—depending

on the detailed dynamics of the stellar debris (see e.g. Refs. [34,35])—a flare is generated, with super-Eddington luminosity that declines with time as $\sim t^{-5/3}$. The flare vanishes rapidly after a time $\Delta T \sim \mathcal{O}(0.1-1)$ yr, when the infall rate drops below the Eddington rate.

Extreme, highly super-Eddington flares are expected if a relativistic jet is launched. The best known jetted TDE is Swift J1644 + 57. Its x-ray flare had an isotropic equivalent luminosity $L_X \simeq 10^{47.5}$ erg s^{-1} over a time interval $\Delta T \simeq 10^6$ s, for a total energy in x rays $E_X = L_X \Delta T \simeq 3 \times 10^{53}$ erg. Note that the applicable luminosity is arguable, as the average (versus peak) luminosity depends on the time interval considered because the luminosity drops with time; see e.g. Ref. [5]. Here we choose the time window and luminosity which we find most appropriate for neutrino production.

A minimum variability time $t_v \sim 10^2$ s was observed in the x-ray luminosity, and a Lorenz factor $\Gamma \sim 10$ for the jet was inferred from the data [8]. The energy E_X is therefore well below the (beaming factor-corrected) maximal isotropic equivalent energy $\sim 2\Gamma^2 E_{\rm max}$. Parameters motivated by Swift J1644 + 57 are considered typical, as they are overall similar to those of the other well established jetted TDE, Swift J2058.4 + 0516 [9].[2] They were used in [17] for neutrino flux estimation, and will be used here as well as a benchmark (see Sec. III B).

B. Rate of TDE

The cosmological rate of TDEs is given by the product of the rate of TDEs per black hole $\dot{N}_{\rm TD}$, the SMBH mass function $\phi(z, M)$, defined as the number of black holes per comoving volume and per unit mass at redshift z, and the occupation fraction, $f_{\rm occ}(M)$, which represents the probability that a SMBH is located at the center of a host galaxy,

$$\dot{\rho}(z, M) = \dot{N}_{\rm TD}(M) f_{\rm occ}(M) \phi(z, M). \quad (6)$$

We describe these quantities following mainly Shankar *et al.* [36], Stone and Metzger [37], and Kochanek [7]. In [36] the black hole mass function is calculated for $M \geq 10^5\ M_\odot$, using information from quasar luminosity functions, and estimates of merger rates to model the growth of black holes. Constraints from local estimates of the black hole mass function are taken into account as well. It is found that $\phi(z, M)$ declines with z—roughly as $(1+z)^{-3}$—and scales approximately like $M^{-3/2}$ for all z and for $10^5\ M_\odot \lesssim M \lesssim 10^{7.5}$.

The occupation fraction $f_{\rm occ}$ can be modeled in the first approximation as a step function, with $f_{\rm occ} \simeq 1$ ($f_{\rm occ} \simeq 0$) above (below) a cutoff mass $M_{\rm min}$. Below this mass a number of effects suppress the probability that low mass SMBH are found in the center of galaxies. For example, a low mass SMBH is more likely to be ejected from the host galaxy; see e.g. [38]. In [37] several possibilities are discussed for the cutoff, with $M_{\rm min} \sim (2 \times 10^5 – 7 \times 10^6)\ M_\odot$. Instead, in [7] the entire mass range $10^5\ M_\odot \lesssim M \lesssim 10^{7.5}\ M_\odot$ is used for the calculation of TDE rates. Even lower mass values, down to $M \simeq 10^{4.5}\ M_\odot$, are considered in [38], motivated by the values of M reported in recent observations of dwarf galaxies [39,40]. We consider the Shankar *et al.* mass function, extrapolated at $M < 10^5\ M_\odot$, and use, for illustration, several values in the interval $M_{\rm min} = (10^{4.5}–10^{6.5})\ M_\odot$ for the cutoff mass.

The rate of tidal disruptions (jetted and nonjetted) per SMBH decreases weakly with increasing M; here we use $\dot{N}_{\rm TD} \simeq 10^{-3.7} (M/10^6\ M_\odot)^{-0.1}$ yr^{-1} [7], which is close to the upper limit obtained from the All-Sky Automated Survey for Supernovae data [41]. We consider only the *total* rate of disruptions per SMBH, neglecting their distribution in the mass of the disrupted star m. As shown in [7], this distribution ranges in the interval $m \sim (0.1–2)\ M_\odot$, with $m \simeq 0.3\ M_\odot$ a typical value. Variations of m in this interval would only produce weak effects (less than a factor of $\sim$2) in our calculations [see Eqs. (1) and (2)]. These effects are subdominant compared to those of M varying over 2 orders of magnitude, and therefore they are neglected here.[3]

Figure 1 shows the differential TDE rate, $\dot{\rho}(z, M) \propto M^{-1.6}$ (left), and the total rate $R(z) = \int_{M_{\rm min}}^{M_{\rm max}} \dot{\rho}(z, M) dM$, as a function of z (right). As expected, $R(z)$ is dominated by the lowest mass SMBH, decreasing by a factor $\sim 10^{0.6} \simeq 4$ when $M_{\rm min}$ is increased by an order of magnitude.

Consider the effective rate of observable jetted TDEs $\tilde{R}$, which can be estimated as $\tilde{R} = R\eta/(2\Gamma^2)$ with the beaming factor $1/(2\Gamma^2)$ and the fraction η of all TDE s producing a jet. Using $\Gamma \simeq 10$ [8] and $\eta \sim 0.1$ [8], the suppression factor between observable jetted and all TDE s can be estimated to be $\sim 5 \times 10^{-4}$. Consequently, the local rate of observable jetted TDE s is expected to be $\tilde{R}(0) \simeq 0.35–10$ Gpc^{-3} yr^{-1}, depending on $M_{\rm min}$. Note that this rate is still subject to possible selection biases if one compares it to data.

It is interesting to compare the expected jetted TDE rate $\tilde{R}(0)$ to constraints from current IceCube data [28–30]. For example, Ref. [29] discusses the case of transient sources, under the assumption that they contribute to most of the astrophysical neutrino flux observed at IceCube. The main result is that rare but powerful transients, with a local rate $\tilde{R}(0) < 10$ Gpc^{-3} yr^{-1}, can be excluded within five years of operation (corresponding to present data) from the

[2]Note, however, that for Swift J2058.4 + 0516, noise limited the sensitivity to time variability to scales larger than $\sim 10^3$ s. The smallest time scale of variability observed was at the level of $\sim 10^4$ s [9].

[3]Note also that the mass of the disrupted star, m, does not directly enter our calculation, where we use observed values of the x-ray luminosity and total energy, L_X and E_X, as inputs; see Sec. III A.

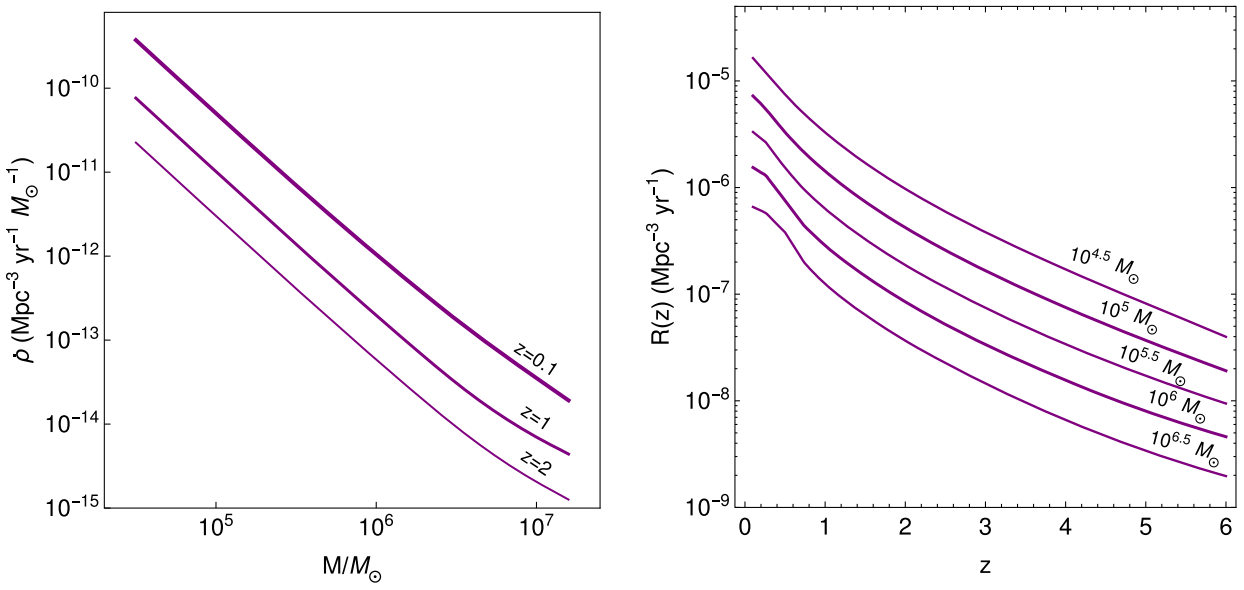

FIG. 1. Left panel: The differential rate of TDEs (jetted and not jetted) $\dot{\rho}(z, M)$ as a function of M for selected values of z (labels on curves). The mass interval $[M_{\rm min}, M_{\rm max}] = [10^{4.5}\ M_\odot, 10^{7.2}\ M_\odot]$ is used here. Right panel: The total volumetric rate of TDEs, $R(z)$, for $M_{\rm max} = 10^{7.2}\ M_\odot$ and different values of $M_{\rm min}$ (labels on curves).

nonobservation of multiplets. These bounds apply to short transients (like GRBs); they relax somewhat for longer lived sources like TDEs.[4] However, it is already evident from that estimate that a diffuse neutrino flux from TDEs describing IceCube data must be dominated by the low mass part of the SMBH mass function in order to avoid the tension with these constraints. A next generation instrument [42] will be more sensitive, being able to identify sources that are more frequent but less bright. A bound might be as strong as $\tilde{R}(0) < 10^3\ {\rm Gpc}^{-3}\,{\rm yr}^{-1}$, which can clearly test the TDE hypothesis. We will discuss another way to test the TDE hypothesis, using the flux flavor composition, in Sec. IV B.

III. NEUTRINO PRODUCTION IN A TDE-GENERATED JET

A. Photohadronic processes and neutrino emission

For the computation of the neutrino flux from a single TDE, we follow the relativistic wind description in Ref. [17]. We apply, however, methods as they have been used in state-of-the-art calculations for relativistic winds in GRBs before [43–45] using the NEUCOSMA software. A comparison between the numerical computation used in this study and the analytical estimate can be found in Appendix A. Our standard parameter values are summarized in Table I. We note that the approach in this section could also easily be applied to TDE stacking analyses, for which the required input is listed in Table I (except from η, but including z); in fact, a very similar method has been used for gamma-ray burst stacking in Ref. [46].

The photon spectrum is assumed to fit the observed spectral energy distributions of TDEs described as a broken power law with a spectral break, parametrized in the shock rest frame (SRF) by (we use primed quantities for the SRF)

$$N'_\gamma(\varepsilon') = C'_\gamma \times \begin{cases} \left(\frac{\varepsilon'}{\varepsilon'_{X,\rm br}}\right)^{-\alpha} & \varepsilon'_{X,\rm min} \le \varepsilon' < \varepsilon'_{X,\rm br} \\ \left(\frac{\varepsilon'}{\varepsilon'_{X,\rm br}}\right)^{-\beta} & \varepsilon'_{X,\rm br} \le \varepsilon' < \varepsilon'_{X,\rm max} \\ 0 & \text{else} \end{cases}, \tag{7}$$

where C'_γ is a normalization factor. Typical values can be found in Table I, where $\varepsilon'_{X,\rm br} = \varepsilon_{X,\rm br}(1+z)/\Gamma$, and $\varepsilon'_{X,\rm min}$ and $\varepsilon'_{X,\rm max}$ can be translated from the observed energy band correspondingly. We use the Swift energy band with $\varepsilon_{X,\rm min} \simeq 0.4$ keV and $\varepsilon_{X,\rm max} \simeq 13.5$ keV [8] to define the target photon spectrum, unless noted otherwise. Note that one may define a bolometric correction to that (such as one may extend the target photon spectrum beyond that range), but the increase of the neutrino flux would be small as long as the break energy was sufficiently well covered.

The proton spectrum is assumed to be a cutoff power law with a spectral index $k_p \simeq 2$ expected from Fermi shock acceleration

$$N'_p(E'_p) = C'_p \times \begin{cases} \left(\frac{E'_p}{\rm GeV}\right)^{-k_p} \cdot \exp\left(-\frac{E'^2_p}{E'^2_{p,\rm max}}\right) & E'_p \ge E'_{p,\rm min} \\ 0 & \text{else} \end{cases}. \tag{8}$$

[4]The other references come to similar conclusions, with some dependence on source evolution history, spectral shape, etc.

TABLE I. Parameters used in this work, unless noted explicitly otherwise. These parameters apply to the SMBH frame.

Symbol	Definition	Standard value
t_v	Variability time scale	10^2 s
Γ	Lorentz factor	10
ξ_p	Baryonic loading (energy in protons versus x rays)	10
ξ_B	Magnetic loading (energy in magnetic field versus x rays)	1
k_p	Proton spectral index	2
E_X	Isotropic equivalent energy in x rays	3×10^{53} erg
ΔT	Duration of x-ray flare	10^6 s
$\varepsilon_{X,\mathrm{br}}$	Observed x-ray break energy	1 keV
α	Lower x-ray spectral index $\varepsilon < \varepsilon_{X,\mathrm{br}}$	2/3
β	Higher x-ray spectral index $\varepsilon > \varepsilon_{X,\mathrm{br}}$	2
η	Fraction of TDEs with jet formation (used for diffuse flux)	0.1

The maximal proton energy $E'_{p,\mathrm{max}}$ is determined automatically by balancing the acceleration rate with synchrotron loss and adiabatic[5] cooling rates and comes from the cutoff from acceleration, and we choose $E'_{p,\mathrm{min}} \simeq 1$ GeV. However, for the neutrino production in TDEs the maximal proton energy is not so important as long as $E'_{p,\mathrm{max}} \gtrsim 10^8$ GeV, because the magnetic field effects on the pions and muons will dominate the maximal neutrino energies and the energy budget only logarithmically depends on $E'_{p,\mathrm{min}}$ and $E'_{p,\mathrm{max}}$ for $k_p = 2$. Consequently, the chosen shape of the (superexponential) cutoff, which may be relevant for the description of ultrahigh energy cosmic rays, does not have any impact on the neutrino flux computation.

The isotropic equivalent energy E_X (in erg) is given in the SMBH frame[6] as

$$E_X = \frac{4\pi d_L^2}{(1+z)} S_X \tag{9}$$

in terms of the x-ray fluence S_X (in units of erg cm^{-2}). Note again that this fluence is assumed to be measured in the energy band from 0.4 to 13.5 keV. The isotropic energy E_X can be obtained from the x-ray luminosity by $E_X = L_X \Delta T_{\mathrm{obs}}/(1+z)$. Here we already see one known subtlety: redshift enters here because the observed duration ΔT_{obs} is defined in the observer's frame and E_X and L_X in the SMBH frame. For the computation of the diffuse flux, it will be most convenient to define all quantities in the SMBH frame, including ΔT, t_v, $\varepsilon_{X,\mathrm{br}}$, $\varepsilon_{X,\mathrm{min}}$, and $\varepsilon_{X,\mathrm{max}}$, which means that all TDEs with the same parameters will be alike in the SMBH frame. Practically, we implement that by computing the neutrino fluxes for a TDE that takes place at a very small $z \ll 1$ (where the observer's frame is basically identical with the SMBH frame). This computation gives the neutrino fluence, i.e., the number of neutrinos of a given flavor that reach Earth per unit energy per unit area, $F_\alpha(E)$ ($\alpha = e, \mu, \tau$). For future use, it is convenient to also consider the number of produced neutrinos of a given flavor (after oscillations) per unit energy $Q_\alpha(E)$, which is related to the fluence by $F_\alpha(E) = Q_\alpha(1+z)^3/(4\pi d_L^2)$ [which is $F_\alpha(E) = Q_\alpha/(4\pi L^2)$ for small z with the look-back distance $L \simeq d_L$]. From F_α and Q_α, the fluence of neutrinos for a generic TDE at any redshift z is obtained by the appropriate rescaling. We checked that the difference between the two methods (all parameters alike in the SMBH frame versus the observer's frame) is small.

The isotropic energy can easily be boosted into the SRF by $E'_X = E_X/\Gamma$. Assuming that the emitted photons are coming from the synchrotron emission of electrons (or mainly interact with electrons), the amount of energy in electrons and photons should be roughly equivalent. In a baryonically dominated relativistic wind, we have

$$E'_p \simeq E'_X \xi_p, \tag{10}$$

where ξ_p is the ratio between the proton and x-ray energy—referred to as "baryonic loading."

We compute the photon and proton densities in the SRF defining an "isotropic volume" V'_{iso}, which is the volume of the interaction region in the source frame assuming isotropic emission of the engine. Thus, the assumption of isotropic emission will cancel in the density. Similarly, V'_{iso} is an equivalent volume in the SRF where only the radial direction is boosted, which is given by

$$V'_{\mathrm{iso}} = 4\pi R_C^2 \Delta d' \tag{11}$$

with shell width $\Delta d' \simeq \Gamma c t_v/(1+z)$ obtained from the variability time scale, and the collision radius $R_C \simeq 2\Gamma^2 c t_v/(1+z)$. From Eq. (11) we can then estimate the size of the interaction region as $V'_{\mathrm{iso}} \propto \Gamma^5 t_v^3$, which means that it strongly depends on the Γ factor.

Because of the intermittent nature of TDEs, the total fluence is assumed to be coming from $N \simeq \Delta T/t_v$ such interaction regions. Now one can determine the normalization of the photon spectrum in Eq. (7) from

$$\int \varepsilon' N'_\gamma(\varepsilon') \mathrm{d}\varepsilon' = \frac{E'_X}{N V'_{\mathrm{iso}}} \tag{12}$$

[5]The adiabatic cooling time scale is chosen to be similar to the dynamical time scale, which means that it is implied that the dynamical time scale can limit the maximal energy.

[6]A clarification is due on the definition of frames of reference used here. For brevity, the wording "SMBH frame" will be used to indicate a frame of reference of an observer at rest with respect to the SMBH and located at a distance L from it such that $R_s \ll L \ll c/H_0$. Instead, "observer's frame" indicates the frame of reference of Earth. Energies in the two frames differ by redshift effects.

if one assumes that the target photons can escape from the source. Note that $E_X/N \simeq L_X t_v$, which means that one can use L_X equivalently to define the target photon density or pion production efficiency—as we do in the analytical approach in Appendix A.

Similarly, one can compute the normalization of the proton spectrum in Eq. (8) by

$$\int E'_p N'_p(E'_p) \mathrm{d}E'_p = \xi_p \frac{E'_X}{N V'_{\mathrm{iso}}}. \tag{13}$$

Given that the ratio between magnetic field and x-ray energies is ξ_B, one has in addition[7]

$$U'_B = \xi_B \frac{E'_X}{N V'_{\mathrm{iso}}} \quad \text{or} \quad B' = \sqrt{8\pi \xi_B \frac{E'_X}{N V'_{\mathrm{iso}}}}. \tag{14}$$

Once the proton and photon densities and the magnetic field are determined, the rest of the computation is straightforward. We solve the time-dependent differential equation system for the pion and consequent muon densities, including photo-meson production based on SOPHIA [47] (with an updated method similar to Ref. [48] and first used in Ref. [49]). We also include the helicity-dependent muon decays [50] and the leading kaon production mode. The radiation processes of the secondary pions, muons, and kaons include synchrotron losses, adiabatic losses, and escape through decay, which lead to characteristic cooling breaks different for pions, muons, and kaons, and a transition in the flavor composition [51]; see Appendix A for an analytical discussion.

B. Neutrino fluence from a tidal disruption event

1. Modeling the jet: Inputs and assumptions

Considering that the masses of the black holes responsible for TDEs may vary over more than 2 orders of magnitude, it is natural to expect a certain degree of diversity in the jetted TDEs. Here we estimate how certain parameters of the jet may depend on the SMBH mass. For the sake of generality, we choose parameter scalings that have either an observational basis or a direct connection to fundamental physics.

Let us first discuss three parameters that most influence the neutrino flux: the minimum variability time t_v, the Lorenz factor Γ, and the luminosity L_X. Observations of AGN indicate a mild dependence of Γ on M which is best fit by [52]

$$\Gamma = \left(\frac{M}{10\ M_\odot}\right)^{0.2}. \tag{15}$$

This corresponds to $\Gamma \sim 6$, 10, and 16 for $M = 10^5$, 10^6, and $10^7\ M_\odot$, respectively, which are compatible with observational estimates for Swift J1644 + 57. The relationship in Eq. (15) is consistent [52] with the magnetically arrested accretion flow model [53,54], which predicts Γ to depend on the square of the SMBH spin, which in turn increases with M. Still, it is not known if Eq. (15) applies to the broader set of galaxies (most of them not hosting an active nucleus) of interest here. Therefore, it should be considered as a mere possibility, although theoretically substantiated.

For the minimum variability time, t_v, it is reasonable to make the hypothesis that it be related to the smallest possible time scale available in a black hole, the Schwarzschild "time" τ_s, Eq. (4). Typical values of τ_s are consistent with the variability seen in Swift J1644 + 57, and indeed the hypothesis of a connection to the Schwarzschild time is used in interpretations of Swift J1644 + 57 data to infer the mass of the parent SMBH [8].

Last, we can expect some dependence of L_X on M. Combined data on jetted and nonjetted TDEs are well fit by a luminosity function that scales like the inverse square of L_X [55],[8]

$$\frac{\dot{\rho}(M)}{\Gamma^2(M)} \propto L_X^{-2}, \tag{16}$$

which implicitly gives a scaling $L_X = L_X(M) \propto \Gamma \dot{\rho}^{-1/2}$. Equation (16) is just a possibility. Indeed, it is also possible that x-ray flares from jetted TDEs do not follow the same trend as the ones from nonjetted TDEs (see Fig. 11 of Ref. [55]). There are also different scalings, resulting from theoretical relationships between x-ray luminosity and SMBH mass (e.g. Refs. [31,32]) such as coming from a possible connections between the peak x-ray luminosity and the rate of accretion.

For the purpose of illustrating possible different degrees of dependence of the neutrino flux on the SMBH mass, M, we present results for four scenarios (see Table II):

(i) *Base case*. Here no dependence on M is considered at all, and a single set of jet parameters is assumed to describe all jetted TDE. The parameters are the same as in [17]; see Table I.

(ii) *Weak scaling case*. Here the weak dependence of Γ on M, motivated by AGN observations, is included, Eq. (15). All other parameters are as in the base case, except the variability time, which is taken to be

[7]With this definition of ξ_B, the magnetic loading is slightly different from Ref. [17], which defines the magnetic energy with respect to the wind luminosity (which is a factor of 3 higher than the radiated energy). Their magnetic loading is therefore effectively a factor of 3 higher than ours.

[8]One can substitute the integral over M by one in L_X in the diffuse flux Eq. (17) for $L_X \propto M^\alpha$, in which case one observes that $\dot{\rho}(M)/\Gamma^2(M)$ corresponds to the luminosity distribution function.

TABLE II. Our standard scaling scenarios.

Case	t_v [s]	Γ	L_X [erg/s]	Reference(s)
Base case	10^2	10	3×10^{47}	Table I, Ref. [17]
Weak scaling case	10^3	$\Gamma=(\frac{M}{10\,M_\odot})^{0.2}$	3×10^{47}	Eq. (15), Ref. [52]
Strong scaling case	$t_v\simeq 63\,\frac{M}{10^6\,M_\odot}$	$\Gamma=(\frac{M}{10\,M_\odot})^{0.2}$	3×10^{47}	Eqs. (4) and (15), Ref. [52]
Lumi scaling case	$t_v\simeq 63\,\frac{M}{10^6\,M_\odot}$	$\Gamma=(\frac{M}{10\,M_\odot})^{0.2}$	$3\times10^{47}\,\frac{M}{10^6\,M_\odot}$	Ref. [55] (see text)

$t_v = 10^3$ s (which is more conservative for neutrino production). This value is meant to illustrate a different possibility, relative to the base value in Table I, and is motivated by the *median* (rather than minimum) scale of time variability observed in Swift J1644 + 57.

(iii) *Strong scaling case*. Here both Γ and $t_v \sim \tau_s$ scale with M as given in Eqs. (4) and (15). This means that, in addition to Γ scaling in the weak case, it is assumed that the time variability of the jet is correlated with the period of the lowest stable orbit of the star disrupted by the SMBH.

(iv) *Lumi scaling case*. Here the same scalings as the strong case are used, and additionally the scaling of L_X is included, as in Eq. (16). Explicitly, considering that $\dot{\rho}(M)\propto M^{-1.6}$ and $\Gamma^2\propto M^{0.4}$ [cf. Eq. (15)], Eq. (16) implies that $L_X\propto M$. We therefore take $L_X = 3\times10^{47}M/(10^6\,M_\odot)$ erg s^{-1}, such that the luminosity is the same as in the strong case for the benchmark SMBH mass $M = 10^6\,M_\odot$.

The general effect of the scalings proposed here can be understood by embedding Eqs. (4), (15), and (16) in the analytical formalism in Appendix A. Considering that Γ and/or t_v increase with M, we expect: (i) a decrease of the pion production efficiency $f_{p\gamma}$, and therefore of the neutrino production, with the increase of M. Indeed, $f_{p\gamma}\propto\Gamma^{-4}t_v^{-1}$ [Eq. (A2)], which implies $f_{p\gamma}\propto M^{-0.8}$ ($f_{p\gamma}\propto M^{-1.8}$) in the weak (strong) case; similar results can be found from Eq. (11). This means that smaller SMBH masses imply higher pion production efficiencies. (ii) An increase of the proton, pion, and muon break energies with M, resulting in a hardening of the neutrino spectrum. This is because these energies scale as, respectively, $E_{p,\rm br}\propto\Gamma^2$, $E_{\pi,\rm br}\propto\Gamma^4 t_v$, and $E_{\mu,\rm br}\propto\Gamma^4 t_v$ [Eqs. (A3), (A4), and (A5)]. This means that $E_{p,\rm br}\propto M^{0.4}$ in both scalings, and $E_{\pi,\rm br}, E_{\mu,\rm br},\propto M^{0.8}$ ($E_{\pi,\rm br}, E_{\mu,\rm br},\propto M^{1.8}$) in the weak (strong) case.

When the dependence of L_X on M is included (lumi case), the neutrino flux roughly scales as $\phi\propto L_X f_{p\gamma}\propto M^{0.2}$, thus increasing slightly with M, contrary to the other scenarios considered here.

All our neutrino flux calculations include neutrino oscillations in vacuum, with the exception of Fig. 5 in Appendix A. We have checked that a possible envelope ahead of the jet, caused by debris of the disrupted star, is sufficiently thin that matter-driven flavor conversion is negligible. Because of the extremely long propagation distance, only the effect of averaged oscillations is observable in a detector, and the corresponding flavor conversion probabilities depend only on the mass-flavor mixing matrix, U: $P(\nu_\alpha\to\nu_\beta)=\sum_{i=1}^3|U_{\alpha i}|^2|U_{\beta i}|^2$, where $\alpha,\beta = e,\ \mu,\ \tau$ and $i = 1,\ 2,\ 3$ runs over the neutrino mass eigenstates. We use the standard parametrization of the mixing matrix, with the following values of the mixing angles: $\sin^2\theta_{12}=0.308$, $\sin^2\theta_{23}=0.437$, and $\sin^2\theta_{13}=0.0234$ (see e.g. Ref. [56]).

2. Neutrino fluence at Earth

Figure 2 (left column) shows the fluence, E^2F_μ, of $\nu_\mu+\bar{\nu}_\mu$ (after oscillations) for a single TDE, for the base case and for the scaling scenarios outlined above and for different values of M. The base case result does not depend on M because the neutrino flux is computed using L_X and fixed values of Γ and t_ν.

The weak case with $M = 10^6\,M_\odot$ differs from the base one only for the value of t_v, which is 1 order of magnitude larger. The neutrino fluence is suppressed by roughly the same factor, as expected from the suppression of the pion production efficiency (Sec. III B 1, Appendix A). From the scaling of Γ [Eqs. (15) and (A2)] a suppression by $\sim10^{0.8}\sim7$ is expected for every decade of increase of M; this matches the behavior in Fig. 2 well at low energy. The figure also shows the expected hardening of the neutrino spectrum with increasing M, due to the increase of the break energies (Sec. III B 1).

For the strong case, the result for $M = 10^6\,M_\odot$ is very similar to the base case, due to the nearly identical parameters. As discussed in Sec. III B 1, here the degree of enhancement with the decrease of M is stronger; this means that low mass black holes will strongly dominate the neutrino flux because the time variability of the jet is assumed to be correlated with the period of the innermost stable orbit—which is shorter for smaller SMBH masses. We also observe the expected stronger broadening of the spectrum toward higher energies due to the stronger scaling of the pion and muon break energies. In the lumi scaling scale, the enhancement from small M is compensated by

the scaling $L_X \propto M$, which means that the flux actually increases with M—as discussed above.

In summary, for a single TDE, in most cases, the quantity E^2F_μ (with F_μ the fluence of muon neutrinos) peaks at $E \sim 10^6$–10^7 GeV, with a maximum value $E^2F_\mu \sim 10^{-5}$–few $\times 10^{-3}$ GeV cm^{-2}. In the scenarios with parameter scaling, the neutrino flux increases with decreasing M. In the case of strong scaling, the fluence can be as high as $E^2F_\mu \sim 10^{-1}$ GeV cm^{-2} at $E \sim$ few $\times 10^5$ GeV.

Figure 2 (right column) also illustrates the flavor ratio $f_\mu = F_\mu/(F_e + F_\tau)$ of neutrino flux after flavor mixing in the three models considered here, and selected values of M.

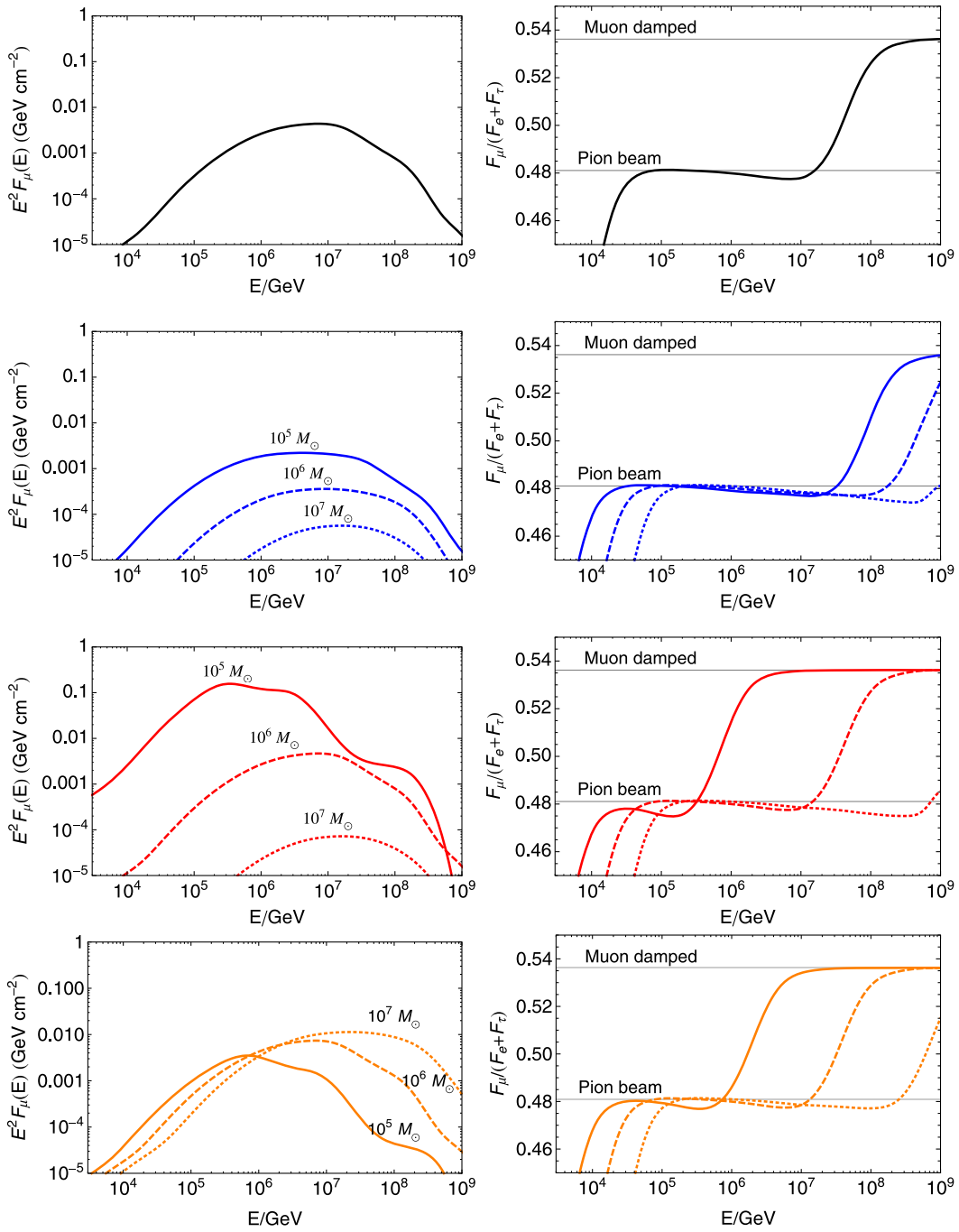

FIG. 2. The fluence of $\nu_\mu + \bar{\nu}_\mu$ (left panels) and the flavor ratio (right panels), including flavor mixing, as a function of the neutrino energy, for a single TDE at $z = 0.35$. Shown are results for the base, weak, strong, and lumi cases (from top to bottom panes). In each panel, the curves correspond to different SMBH masses, $M = 10^5\ M_\odot$ (solid curve), $M = 10^6\ M_\odot$ (dashed curve), and $M = 10^7\ M_\odot$ (dotted curve). For the flavor ratio, the horizontal lines show the values expected for the standard preoscillation compositions $(F_e^0 : F_\mu^0 : F_\tau^0) = (1, 2, 0)$ (pion beam) and $(F_e^0 : F_\mu^0 : F_\tau^0) = (0, 1, 0)$ (muon damped source).

This flavor ratio roughly corresponds to the observable ratio between muon tracks and cascades in IceCube, and it has been widely used in the literature to study the impact of a change of the flavor composition. For all models there is an energy window where $f_\mu \simeq 0.48$; this is the region where μ decay proceeds unimpeded, $E_\mu \gtrsim E_{\mu,\mathrm{br}}$. In this regime, for each pion in the jet, two muon neutrinos and one electron neutrinos are expected, so that the original (before oscillations) flavor composition of the neutrino flux is $(F_e^0 : F_\mu^0 : F_\tau^0) = (1:2:0)$. At higher energy, $E_\mu \gtrsim E_{\mu,\mathrm{br}}$, the ratio f_μ increases to $f_\mu \simeq 0.536$, reflecting the transition to the regime where μ absorption dominates over decay, so that the original flavor content is $(F_e^0 : F_\mu^0 : F_\tau^0) \simeq (0,1,0)$. While $E_{\mu,\mathrm{br}}$ is nearly the same for the base and weak cases, it is much lower for the strong and lumi scenarios at lower M, so that for $M = 10^5\ M_\odot$, already at energies of a few PeV the neutrino flux enters the muon damped regime.

IV. DIFFUSE NEUTRINO FLUX FROM TDE

A. Diffuse flux prediction: Spectrum and flavor composition

The diffuse flux of neutrinos of a given flavor α from TDEs—differential in energy, time, area, and solid angle—is obtained by convolving the neutrino emission of a single TDE with the cosmological rate of TDEs (see e.g. [57] for the formalism),

$$\Phi_\alpha(E) = \frac{c}{4\pi H_0}\int_{M_{\mathrm{min}}}^{M_{\mathrm{max}}} dM \frac{\eta}{2\Gamma^2(M)} \times \int_0^{z_{\mathrm{max}}} dz \frac{\dot{\rho}(z,M) Q_\alpha(E(1+z),M)}{\sqrt{\Omega_M(1+z)^3+\Omega_\Lambda}}, \quad (17)$$

where Q_α is the number of neutrinos emitted per unit energy in the SMBH frame, and $E' = E(1+z)$ is the neutrino energy in the same frame; E is the energy observed at Earth. Here η is the fraction of TDEs that generate relativistic jets, which is assumed to be a constant, $\eta \simeq 0.1$. This value has been suggested as plausible on the basis of a possible similarity with AGN [8]. The beaming factor $1/(2\Gamma^2(M))$ accounts for the fraction of jets along our line of sight. Its use in Eq. (17) is consistent with the fact that the same equation contains the physical comoving rate of TDEs (not corrected for beaming or observational biases). Because of the decline of $\dot{\rho}(z,M)$ with z (Fig. 1), the flux Φ_α depends only weakly on z_{max}; here we take $z_{\mathrm{max}} = 6$, which is the maximum value considered in SMBH mass function calculation of Shankar *et al.* [36].

Figure 3 shows the diffuse muon neutrino flux, $E^2\Phi_\mu(E)$, for the four scaling scenarios of interest, and $M_{\mathrm{min}} = 10^5,\ 10^6\ M_\odot$ (solid curves). The shaded area models the uncertainty on M_{min}, which is varied in the interval $M_{\mathrm{min}} = [10^{4.5}, 10^{6.5}] M_\odot$. In all cases, the spectrum resembles the spectrum of a single TDE with $M \sim M_{\mathrm{min}}$ and $z \ll 1$ (Fig. 2), as expected since the TDE rate is a decreasing function of z and M (Fig. 1). For the base, weak, and lumi cases (with $M_{\mathrm{min}} = 10^5\ M_\odot$), the diffuse flux has a maximum of $E^2\Phi_\mu(E) \sim 10^{-9}\,\mathrm{GeV\,cm^{-2}\,s^{-1}\,sr^{-1}}$ between 1 PeV and 10 PeV. For the weak case, we note the stronger contribution of the lowest mass SMBH, $M = 10^5$–$10^6\ M_\odot$, reflecting the more powerful neutrino emission as M decreases (Sec. III B). The same features are observed for the strong case, with an even more enhanced contribution of the lowest mass SMBH, which causes the flux to peak at lower energy, $E \sim 0.3$ PeV. The dependence on M_{min} is, on the other hand, relatively mild for the base and lumi cases.

The postoscillation flavor ratio for the diffuse flux is shown in Fig. 3 (right column). Like the fluence, it mainly follows the corresponding quantity for a single TDE with lowest M and lowest z (Fig. 2). In the lumi case, the contributions from lower and higher M are comparable at about 10 PeV. The observational implications of the energy dependence of the flavor composition will be discussed in the next section.

Before closing this section, let us briefly comment on constraints on TDEs from x-ray surveys. As a consistency check, in Appendix B we present the diffuse x-ray flux corresponding to the four scaling scenarios in Table II. This flux is found to be consistent with observations (see Appendix B).

B. Comparison to IceCube data

Let us now discuss the impact of current and future IceCube data on the search for neutrinos from TDEs. After about six years of data taking, IceCube has established that the Earth receives a flux of astrophysical neutrinos which is diffuse in nature, in first approximation, and at the level of $E^2\Phi \sim \text{few} \times 10^{-8}\ \mathrm{GeV\,cm^{-2}\,s^{-1}\,sr^{-1}}$, at observed energies between ~30 TeV and ~PeV. Even accounting for large and poorly known uncertainties—which depend in part on the model of the candidate sources—this measurement appears to be in tension with the most extreme flux predictions in Fig. 3. In particular, for the parameters of reference used in this work, the strong scaling scenario with $M_{\mathrm{min}} \sim 10^{4.5}$–$10^5\ M_\odot$ should already be strongly disfavored by the IceCube data, whereas all the other cases are compatible with IceCube observations.

One should consider, however, that the jet parameters have a wide range of plausible values, which leads to a more quantitative question: can TDEs account for most of the IceCube flux, and for what values of the parameters? From Eqs. (13) and (17) we see that Φ_μ scales directly with

$$G \equiv \xi_p \times \eta \simeq 10 \times 0.1 \simeq 1, \quad (18)$$

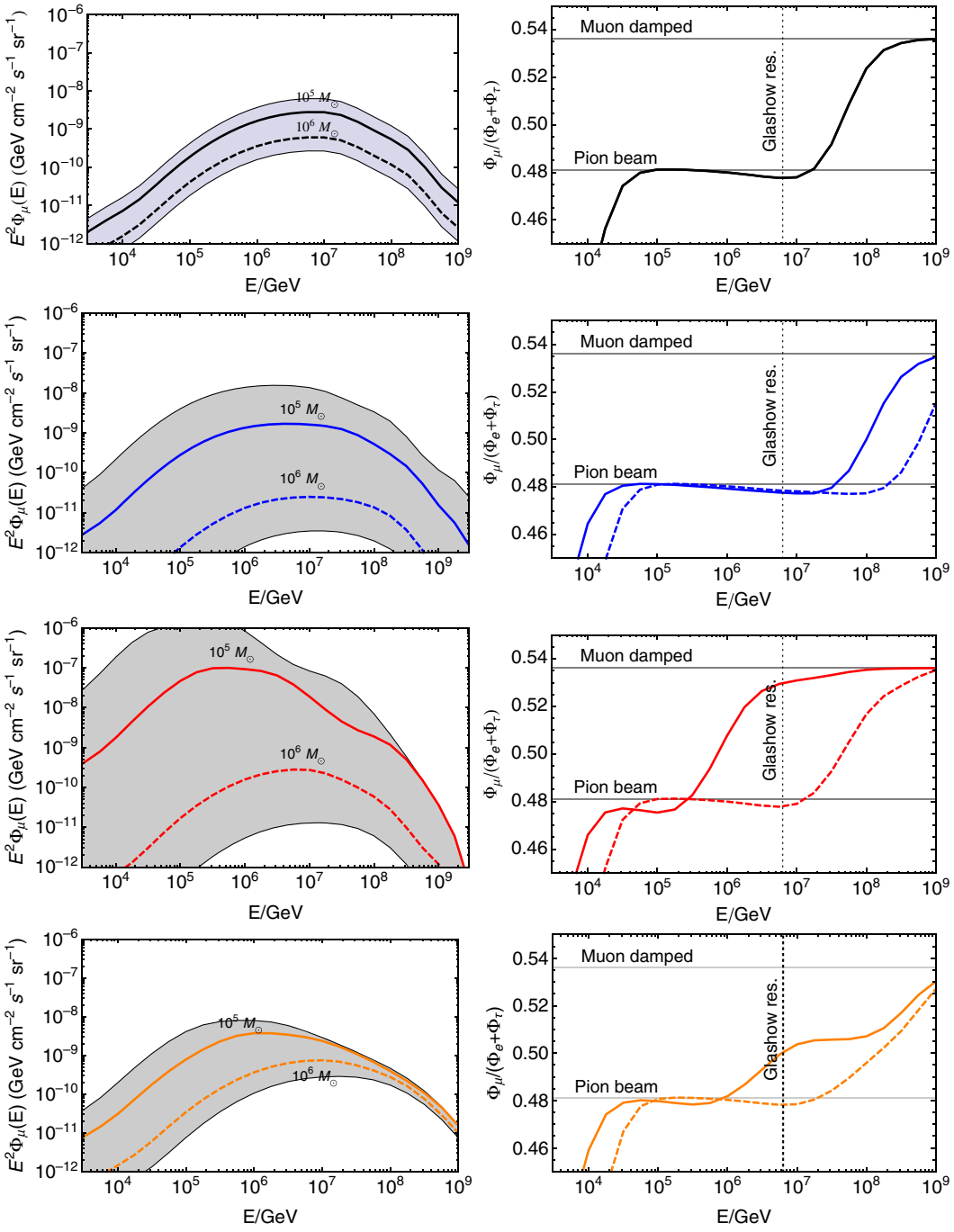

FIG. 3. The diffuse flux of $\nu_\mu + \bar{\nu}_\mu$ (left panes) and the corresponding flavor ratio (right panes) at Earth, including flavor mixing, as a function of the neutrino energy, for the base, weak, strong, and lumi scaling cases (top to bottom), for $M_{\rm min} = 10^5\ M_\odot$ (solid curves), and $M_{\rm min} = 10^6\ M_\odot$ (dashed curves). In the flux plots, the shaded regions show the variation corresponding to varying $M_{\rm min}$ in the interval $M_{\rm min} = [10^{4.5}, 10^{6.5}]M_\odot$. In the flavor ratio figures, the horizontal lines show the values expected for the standard preoscillation compositions $(\phi_e^0 : \phi_\mu^0 : \phi_\tau^0) = (1, 2, 0)$ (pion beam) and $(\phi_e^0 : \phi_\mu^0 : \phi_\tau^0) = (0, 1, 0)$ (muon damped source). The energy of the Glashow resonance in the flavor composition panels is marked by a dotted line.

evaluated for our standard assumptions. In principle, the neutrino flux also scales with the x-ray luminosity (as both the initial proton and the pion production efficiency are proportional to L_X), the beaming factor, the minimal and maximal proton energies (as the proton total energy is distributed over that energy range), etc. However, these scaling factors are less trivial to treat, as, for instance, a higher luminosity will increase not only the pion

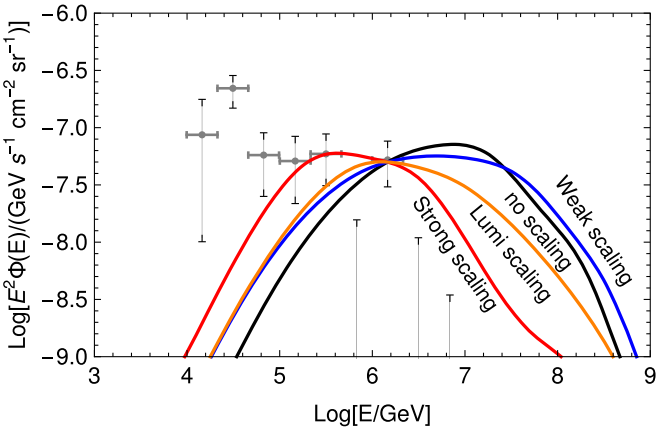

FIG. 4. The spectra for the diffuse all-flavor flux, for the strong, weak, lumi, and base (i.e., no scaling) models (labels on curves), for $M_{\rm min} = 10^5\ M_\odot$. The overall constant $G = \xi_p \times \eta$ has been adjusted to saturate the measured IceCube flux at $E \simeq$ PeV (shown, data points [58,59]), and takes the values $G = 0.2$, 10.9, 4.3, 8.1 for the strong, weak, lumi, and base cases, respectively.

production but also the magnetic field and therefore the secondary cooling—which partially compensates for that. We therefore do not include them directly in G.

Figure 4 shows the all-flavor fluence for the diffuse flux, for $M_{\rm min} = 10^5\ M_\odot$, with the factor G adjusted (values in the figure caption) to saturate the IceCube data (shown as well) at $E \simeq 1$ PeV. Note that we do not perform a statistical analysis of the data, but rather the normalization of the predicted flux is chosen so that the data point at 1 PeV is exactly reproduced. We see that the base and weak cases can describe the data in the 0.1–1 PeV energy range, although at the price of invoking parameter values $G \sim$ 8–11. Such an increase of the neutrino flux could come from a factor of 10 higher baryonic loading than anticipated in Table I, i.e., $\xi_p \sim 100$, or, equivalently, from a higher value of η.

Such a large baryonic loading may on the one hand not be unreasonable, as similar values are found for gamma-ray bursts fitting the Ultra-high energy cosmic ray data [60]. In our notation, one can easily compare the energy in baryons with the constraint on the energy Eq. (5): For the chosen E_X and the conservative estimate $\Gamma \gtrsim 6$ (for $M > 10^5\ M_\odot$), one finds $\xi_p \lesssim 2\Gamma^2 E_{\rm max}/E_X \sim 200$ in order not to violate the constraint on the maximal emitted energy. This constraint is satisfied here, but the jets will have to be dominated by baryons for low mass black holes. However, increasing ξ_p versus η has the problem that it increases the tension with the multiplet constraints in IceCube, whereas increasing η versus ξ_p changes the fraction of jetted versus nonjetted TDEs. In addition to requiring a somewhat extreme value of ξ_p, the base and weak cases are in overall tension with the data due to their relatively hard spectrum, which overestimates the flux above PeV while underestimating it at lower energy. Our nominal assumptions may therefore be more plausible. In different words, for the base case, we find that $1/8 \simeq 12\%$ of the observed flux in IceCube can be described by TDEs, whereas we find $1/11 \simeq 9\%$ for the weak case at an energy of about 1 PeV.

Instead, the strong case describes data best: it reproduces the observed energy spectrum well, with only some tension with the data in the second lowest energy bin, and only slightly overestimating the flux at the highest energy; see Fig. 4. The normalization leads to $G \simeq 0.2$, i.e., parameters even more conservative than the reference values used in Eq. (18). For example, one may choose $\xi_p = 2$ and $\eta = 0.1$, or $\xi_p = 10$ and $\eta = 0.02$. Regarding the spectral properties, one should keep in mind that in this scenario the neutrino flux is vastly dominated by the lowest mass black holes (see Fig. 3, lower left panel), with a strong dependence on $M_{\rm min}$. For smaller $M_{\rm min}$, $M_{\rm min} \sim 10^{4.5}\ M_\odot$, the description of data becomes better due to the softening of the neutrino spectrum, and the value of G required to saturate the measured flux decreases further. The opposite effect (worse description of data) is expected for larger $M_{\rm min}$.

The lumi scaling case is found to be in between these two scenarios. At the nominal prediction, 23% of the observed IceCube flux can be described by TDEs. The flux can, however, be saturated if the baryonic loading or η are slightly adjusted, such as $\xi_p \simeq 40$ and $\eta = 0.1$. The spectrum describes IceCube data with slightly larger cutoff energy.

It is interesting to compare our prediction to current IceCube data fits. For a global analysis of data [59], relatively soft spectral indices of the neutrinos are found: $\alpha \simeq 2.5$ for a power law fit. A recent throughgoing muon analysis, however, indicates a spectral index $\alpha \simeq 2$ [61]. These findings, together with information on the spatial distribution of the events, suggest the possibility that at low energies a softer, possibly Galactic contribution dominates (cf. low energy data points in Fig. 4, which cannot be reproduced), whereas at high energy, an extragalactic component dominates and the spectrum becomes harder [62,63]. The diffuse flux from TDEs is an example for such an extragalactic hard component.

It is especially noteworthy that the strong and lumi scaling cases have a unique signature, apart from the good description of the spectral shape: in this case the flavor composition changes from a pion beam to a muon damped source at $E \sim$ PeV (see lower right panels of Fig. 3). This indicates the transition to a regime, as the energy increases, where muons cool faster by synchrotron losses than they can decay; see Eq. (A5). While this effect can probably not be seen in the current IceCube experiment, it might be visible at the planned volume upgrade IceCube-Gen2 [42]; see Ref. [64] (Figs. 3 and 9 there).

Perhaps even easier to test is the fact that the diffuse flux becomes muon damped at the Glashow resonance; see vertical lines in the right panels of Fig. 3. This issue is discussed in Ref. [65]: if the spectrum is hard enough,

Glashow events must be seen in the current IceCube experiment after about 10 years of operation even in the $p\gamma$ case under realistic assumptions for the photohadronic interactions. The most plausible scenario which can evade this constraint is a muon-damped source at the Glashow resonance at 6.3 PeV, for which the $\bar{\nu}_e$ at Earth can only come from oscillated $\bar{\nu}_\mu$ from the π^- contamination at the source. A nonobservation of Glashow event rates in IceCube may therefore be a smoking gun signature for a muon damped source at the Glashow energy, and therefore TDEs as dominant source class—or alternatives, such as low-luminosity gamma-ray bursts [66], microquasars [67], or AGN nuclei [26]. IceCube-Gen2 can then be used for more detailed source diagnostics.

V. SUMMARY AND CONCLUSIONS

We have studied the production of high energy neutrinos in baryonic jets generated in the TDEs of stars by SMBH. Using the NEUCOSMA numerical package, detailed results have been obtained for the fluence and flavor composition of a neutrino burst from an individual TDE, and for the diffuse flux of neutrinos of each flavor from all cosmological TDEs. Jet parameters motivated by observations have been used, and variations of these parameters over the diverse population of parent SMBH—in the form of scalings with the SMBH mass M—have been studied. Four scaling scenarios have been considered, ranging from no scaling at all (all TDE being identical in the SMBH frame) to a strong scaling, where the bulk Lorentz factor Γ has been varied in a way motivated by AGN observations, and the variability time scale t_v has been assumed to be correlated with the innermost stable orbital period of the SMBH. We have also considered a possible luminosity distribution function, related to the SMBH mass distribution. The dependence on the occupation fraction of SMBH—in the form of the minimum mass $M_{\rm min}$ of SMBH that can be found in the core of galaxies—has been studied as well.

In summary, we find the following:

(i) The largest contribution to the diffuse neutrino flux is expected from the SMBH with the lower mass located at low redshift $z \lesssim 1$. This is because the rate of TDEs decreases with M, and with z as well. The dominance of low M TDEs is stronger in the scenarios with parameter scaling, as discussed above, and weakened if the luminosity scales with SMBH mass. In all cases, the spectral features and flavor composition of the diffuse flux generally reflect the quantities of the lowest mass SMBH, and therefore are very sensitive to the cutoff of the SMBH occupation fraction, $M_{\rm min}$.

(ii) For the jet parameters of reference (Table 1), and in cases with weak or no scaling, TDEs can be responsible for ~10% of the observed neutrino flux at IceCube at an energy of about 1 PeV. Instead, for the same parameters, strong scaling, and $M_{\rm min} \lesssim 10^5\ M_\odot$, the nominal neutrino flux would exceed the IceCube measurement, which means that this extreme situation is already disfavored by current data, and IceCube constrains $M_{\rm min}$, the baryonic loading ξ_p, and the fraction η of TDE producing jets.

(iii) As a consequence, more moderate parameters can be chosen for the strong scaling case—which can describe both normalization and spectral shape of the observed diffuse flux at the highest energies. Examples are $\eta = 0.1$ and $\xi_p = 2$, or $\eta = 0.02$ and $\xi_p = 10$. Note that more frequent TDEs with lower baryonic loadings can release a possible tension with constraints from the nonobservation of neutrino multiplets. We also find that a second, possibly softer, contribution to the flux of a different origin (possibly Galactic) is needed to account for the lowest energy neutrino events.

(iv) For the strong scaling case, which describes the spectral shape best, the flavor composition changes with increasing energy and approaches a muon damped source at $E \gtrsim$ PeV. This signature may be detectable in the next generation upgrade IceCube-Gen2. In addition, recall that so far IceCube has not observed any events at the Glashow resonance. If this became a statistically significant suppression in the future, it could be a smoking gun signature for TDEs as a dominant source, because it is expected for a muon damped source.

(v) If the luminosity of jetted TDEs scales with the SMBH mass—in addition to the scalings of the Lorentz factor and of the variability time scale—an intermediate case is found which describes the spectrum very well, which exhibits a flavor composition change at the Glashow resonance, and which can describe about one-fourth of the observed diffuse IceCube flux at its nominal prediction—or saturate the diffuse flux with a slight increase of ξ_p or η. This case corresponds to a x-ray luminosity distribution function $\propto L_X^{-2}$ (Sec. III B 1).

Overall, we find TDEs to be an attractive possibility to explain, at least in part, the still elusive origin of the observed neutrino flux. Indeed, they naturally fit a hypothesis that has recently emerged from data analyses: that the IceCube signal might be due to relatively frequent, transient photohadronic sources with photon counterparts at sub-MeV energies only. Upcoming, higher statistics data at IceCube and its future evolutions (such as IceCube-Gen2) could substantiate the TDE hypothesis in a number of ways. One could be dedicated searches for time and space correlations of neutrino events with known TDEs, possibly to be done in collaboration with astronomical surveys. Another way is more detailed studies of the diffuse flux that could show transitions as the energy increases, in the spectral index and flavor composition of the flux, thus

indicating the presence of a distinct component at ∼PeV, of a different origin than the lower energy events.

Of course, one should consider the large uncertainties that affect the prediction of the neutrino flux from TDEs. We illustrated some of them, especially those due to the uncertain low mass cutoff (i.e., the lower mass end of the SMBH occupation fraction), and those associated with the scaling of time variability or of the Lorentz factor of the jet with the SMBH mass, the baryonic loading of the jet, the fraction of TDEs producing jets, and the uncertain luminosity distribution. These quantities are likely to become better known as more astronomical data are gathered on TDEs.

It is also fascinating that neutrino detectors themselves might contribute to our learning of the physics of tidal disruption. Indeed, flux constraints from neutrino data could establish important upper limits on the energetics, baryon content, and frequency of TDEs; these limits would be complementary to astronomical observations, which are more strongly affected by absorption and limited sky coverage. Alternatively, a discovery of TDEs as neutrino sources would most likely give upper limits on the low black hole mass cutoff and would distinguish among different scaling models for the jet parameters with the black hole mass. By probing tidal disruption events, neutrino data would therefore contribute to answering unresolved questions on the fundamental physics of black holes, on the birth and evolution of supermassive black holes, and on the dynamics of galactic cores that are usually quiet and are only "illuminated" occasionally by tidal disruption.

ACKNOWLEDGMENTS

We thank M. Ahlers, L. Dai, A. Franckowiak, M. Kowalski, K. Murase, A. Stasik, and N. L. Strotjohann for useful discussions. C. L. is grateful to the DESY Zeuthen laboratory for hospitality when this work was initiated. She acknowledges funding from Deutscher Akademischer Austausch Dienst (German Academic Exchange Service), the National Science Foundation Grant No. PHY-1205745, and the Department of Energy Grant No. DE- SC0015406. W. W. acknowledges funding from the European Research Council (ERC) under the European Union's Horizon 2020 research and innovation program (Grant No. 646623).

Note added.—During completion of this study, Refs. [68,69] appeared. Their conclusions (about 5%–10% of the diffuse flux observed at IceCube could be consistent with the TDE hypothesis) are roughly consistent with our result for the base case ($1/8.12 \simeq 12\%$). The authors of Ref. [68] compute event rates from individual TDEs and derive a constraint on the diffuse IceCube flux. The authors of Ref. [69] also consider neutrinos from chocked jets and conclude that the contribution must be subdominant. Note that their $\tilde{\xi}_{\rm cr}$ corresponds to our ξ_p. Compared to Refs. [68,69], our work includes a fully numerical computation of the diffuse flux including flavor effects, and the scaling assumptions with the SMBH mass function are unique to our work.

APPENDIX A: COMPARISON TO AN ANALYTICAL COMPUTATION

Here we compare our numerical computation to the analytical approach given in Ref. [17]. We assume the same parameters as in Table I and the main text, unless explicitly stated. The following relationships among the observables are assumed to hold at $z = 0$, where the observer's frame corresponds to the SMBH frame.

It is reasonable to approximate the pion, muon, and neutrino energies as fixed fractions of the parent proton energy, $E_\pi \sim 0.2E_p$, $E_\mu \sim 0.15E_p$, and $E \sim 0.05E_p$. The neutrino flavor fluences (without flavor mixings) can be modeled analytically as [17]

$$E^2F^0_\mu(E) = \frac{1}{32\pi d_L^2}\frac{E_X\xi_p}{\ln(E_{p,\rm max}/E_{p,\rm min})} f_{p\gamma}\zeta_\pi(1+\zeta_\mu),$$
$$E^2F^0_e(E) = \frac{1}{32\pi d_L^2}\frac{E_X\xi_p}{\ln(E_{p,\rm max}/E_{p,\rm min})} f_{p\gamma}\zeta_\pi\zeta_\mu. \quad \text{(A1)}$$

The pion production efficiency $f_{p\gamma}$ is the average fraction of energy deposited into pion production. It is, similar to gamma-ray bursts [70,71], given by

$$f_{p\gamma} \simeq 0.35\left(\frac{L_X}{10^{47.5}\,\rm erg\ s^{-1}}\right)\left(\frac{\Gamma}{10}\right)^{-4}\left(\frac{t_v}{10^2\ \rm s}\right)^{-1}\left(\frac{\epsilon_b}{\rm KeV}\right)^{-1} \times \begin{cases} (E_p/E_{pb})^{\beta-1} & \text{for } E_p < E_{p,\rm br} \\ (E_p/E_{pb})^{\alpha-1} & \text{for } E_p \geq E_{p,\rm br} \end{cases}. \quad \text{(A2)}$$

Here $L_X = E_X/\Delta T$ is the average x-ray luminosity, and $E_{p,\rm br}$ is the proton energy leading to photopion production at the Δ resonance corresponding to the x-ray break energy, i.e.,

$$E_{p,\rm br} = 1.5\,10^7\ \rm GeV\left(\frac{\Gamma}{10}\right)^2\left(\frac{1\ \rm KeV}{\epsilon_{X,\rm br}}\right). \quad \text{(A3)}$$

In Eq. (A1), the factors ζ_π and ζ_μ are suppression factors that account for pion and muon propagation (energy losses and decay). The quantity ζ_π can be expressed in terms of a spectral break energy $E_{\pi,\rm br}$, beyond which the time scale of synchrotron losses becomes smaller than the pion lifetime,

$$\begin{cases} \zeta_\pi = 1 & \text{for } E_\pi \lesssim E_{\pi,\rm br} \\ \zeta_\pi \propto E_\pi^{-2} & \text{for } E_\pi \gtrsim E_{\pi,\rm br} \end{cases} \text{ with}$$
$$E_{\pi,\rm br} \simeq 5.8\times 10^8\ \rm GeV\left(\frac{L_X}{10^{47.5}\ \rm erg\,s^{-1}}\right)^{-\frac{1}{2}}\left(\frac{\xi_B}{1}\right)^{-\frac{1}{2}} \times \left(\frac{\Gamma}{10}\right)^4\left(\frac{t_v}{10^2 s}\right). \quad \text{(A4)}$$

A similar expression holds for ζ_μ, for with

$$E_{\mu,\mathrm{br}} \simeq 3.1 \times 10^7 \ \mathrm{GeV} \left(\frac{L_X}{10^{47.5} \mathrm{erg\,s^{-1}}}\right)^{-\frac{1}{2}} \left(\frac{\xi_B}{1}\right)^{-\frac{1}{2}} \times \left(\frac{\Gamma}{10}\right)^4 \left(\frac{t_v}{10^2 s}\right). \quad \text{(A5)}$$

A comparison between the analytical technique and the numerical techniques is given in Fig. 5. First of all, it is noteworthy that our numerical and analytical techniques match relatively well in terms of both shape and normalization.

The slightly different shape comes mostly from high-energy photohadronic processes (see Ref. [43]), from kaon production (at the highest energies), and from the different treatment of the photoproduction threshold (at the breaks) [45]. At low neutrino energies, the analytical curves are simply extrapolated with Eq. (A2) using the high-energy photon spectral index β, whereas the numerical computation cuts off at a maximal photon energy given by the observed energy window (relevant for the minimal neutrino energy).

The somewhat lower numerical versus analytical normalization is rather a coincidence of two competing processes: additional (to the Δ resonance) high-energy photomeson production modes enhance the pion production compared to the analytical estimate and make the spectral peaks more pronounced [43], whereas several reduction factors have been identified in Refs. [45,72]. One example for the flux reduction is the overestimation of the pion production efficiency using the break energy in Eq. (A2) instead of integrating over the whole spectrum. The relative normalization between analytical and numerical computation depends on the type of assumptions made for the analytical computation and the parameters (such as photon break energy and spectral indices).

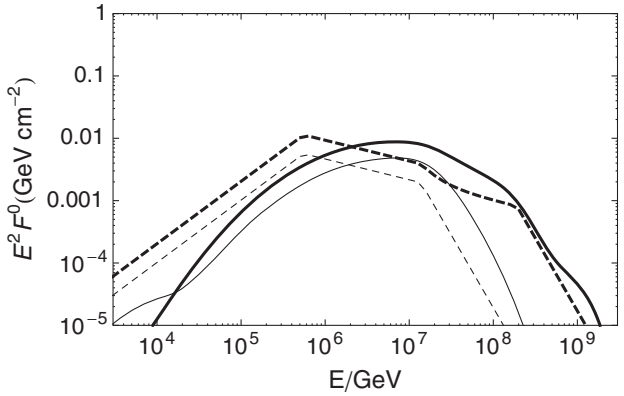

FIG. 5. The fluence $E^2F^0_\alpha$ for $\nu_\mu + \bar{\nu}_\mu$ ($\alpha = \mu$, thick curve) and $\nu_e + \bar{\nu}_e$ ($\alpha = e$, thin curve), for a TDE at $z = 0.35$. Dashed lines: analytical approximation; solid lines: NEUCOSMA numerical result. Flavor mixing is not included here, hence the factor of ~2 difference in the fluence compared to Fig. 2.

We observe that the analytical method matches the numerical computation relatively well (within about a factor of 2), whereas for GRBs, the analytical computation typically overestimates the neutrino flux much more significantly.

APPENDIX B: PREDICTED X-RAY FLUX

As a consistency check of our results, we calculated the x-ray flux expected for the different scaling scenarios (Table II), following the same formalism as in Eq. (17). The results are shown in Fig. 6. As expected from the scalings of Γ and L_X, the contribution of the lower mass SMBH is largest in the weak and strong cases, and suppressed in the lumi case. Note that the weak and strong

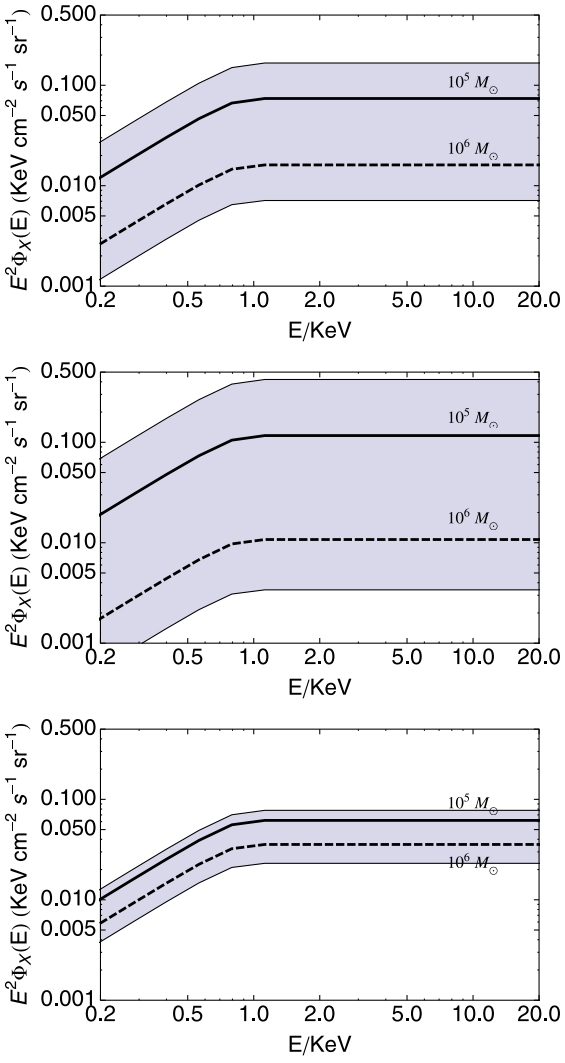

FIG. 6. The diffuse x-ray flux predicted in the base case (upper pane), weak and strong cases (middle pane), and lumi case (lower pane), for $M_{\min} = 10^5\ M_\odot$ (solid lines), and $M_{\min} = 10^6\ M_\odot$ (dashed lines). The shaded regions show the variation corresponding to varying $M_{\min}$ in the interval $M_{\min} = [10^{4.5}, 10^{6.5}] M_\odot$.

cases differ only by t_v, which affects the neutrino production but not the x-ray flux. In all scenarios, the flux is consistent with observations, being at least 1 order of magnitude below the diffuse extragalactic soft x-ray flux as measured at $E \simeq 0.25$ KeV by ROSAT: $E^2\Phi_X \simeq$ 5–9 KeV cm^{-2} s^{-1} sr^{-1} [73]. At $E \gtrsim$ KeV, the observed diffuse flux is even larger (see e.g. [74] and references therein), thus strongly outshining the predicted TDE flux.

[1] J. G. Hills, Nature (London) **254**, 295 (1975).
[2] M. J. Rees, Nature (London) **333**, 523 (1988).
[3] J. H. Lacy, C. H. Townes, and D. J. Hollenbach, Astrophys. J. **262**, 120 (1982).
[4] E. S. Phinney, in The Center of the Galaxy, *IAU Symposium Proceedings* Vol. 136, edited by M. Morris (Kluwer Academic Publishers, Dordrecht, 1989), p. 543.
[5] K. Auchettl, J. Guillochon, and E. Ramirez-Ruiz, Astrophys. J. **838**, 149 (2017).
[6] S. Komossa, J. High Energy Astrophys. **7**, 148 (2015).
[7] C. S. Kochanek, Mon. Not. R. Astron. Soc. **461**, 371 (2016).
[8] D. N. Burrows *et al.*, Nature (London) **476**, 421 (2011).
[9] S. B. Cenko *et al.*, Astrophys. J. **753**, 77 (2012).
[10] G. C. Brown, A. J. Levan, E. R. Stanway, N. R. Tanvir, S. B. Cenko, E. Berger, R. Chornock, and A. Cucchiaria, Mon. Not. R. Astron. Soc. **452**, 4297 (2015).
[11] S. van Velzen *et al.*, Science **351**, 62 (2016).
[12] W.-H. Lei, Q. Yuan, B. Zhang, and D. Wang, Astrophys. J. **816**, 20 (2016).
[13] A. J. Levan, J. High Energy Astrophys. **7**, 44 (2015).
[14] G. R. Farrar and A. Gruzinov, Astrophys. J. **693**, 329 (2009).
[15] G. R. Farrar and T. Piran, arXiv:1411.0704.
[16] D. N. Pfeffer, E. D. Kovetz, and M. Kamionkowski, Mon. Not. R. Astron. Soc. **466**, 2922 (2017).
[17] X.-Y. Wang, R.-Y. Liu, Z.-G. Dai, and K. S. Cheng, Phys. Rev. D **84**, 081301 (2011).
[18] X.-Y. Wang and R.-Y. Liu, Phys. Rev. D **93**, 083005 (2016).
[19] K. Murase and K. Ioka, Phys. Rev. Lett. **111**, 121102 (2013).
[20] M. Aartsen *et al.* (IceCube Collaboration), Science **342**, 1242856 (2013).
[21] M. G. Aartsen *et al.* (IceCube Collaboration) Astrophys. J. **835**, 45 (2017).
[22] R. Abbasi *et al.* (IceCube Collaboration), Nature (London) **484**, 351 (2012).
[23] M. G. Aartsen *et al.* (IceCube Collaboration), Astrophys. J. **805**, L5 (2015).
[24] K. Murase, M. Ahlers, and B. C. Lacki, Phys. Rev. D **88**, 121301 (2013).
[25] K. Bechtol, M. Ahlers, M. Di Mauro, M. Ajello, and J. Vandenbroucke, Astrophys. J. **836**, 47 (2017).
[26] W. Winter, Phys. Rev. D **88**, 083007 (2013).
[27] K. Murase, D. Guetta, and M. Ahlers, Phys. Rev. Lett. **116**, 071101 (2016).
[28] M. Kowalski, J. Phys. Conf. Ser. **632**, 012039 (2015).
[29] M. Ahlers and F. Halzen, Phys. Rev. D **90**, 043005 (2014).
[30] K. Murase and E. Waxman, Phys. Rev. D **94**, 103006 (2016).
[31] F. De Colle, J. Guillochon, J. Naiman, and E. Ramirez-Ruiz, Astrophys. J. **760**, 103 (2012).
[32] J. Guillochon and E. Ramirez-Ruiz, Astrophys. J. **767**, 25 (2013); **798**, 64(E) (2015).
[33] G. E. Romero and G. S. Vila, Lect. Notes Phys. **876**, 1 (2014).
[34] H. Shiokawa, J. H. Krolik, R. M. Cheng, T. Piran, and S. C. Noble, Astrophys. J. **804**, 85 (2015).
[35] L. Dai, J. C. McKinney, and M. C. Miller, Astrophys. J. **812**, L39 (2015).
[36] F. Shankar, D. H. Weinberg, and J. Miralda-Escude, Astrophys. J. **690**, 20 (2009).
[37] N. C. Stone and B. D. Metzger, Mon. Not. R. Astron. Soc. **455**, 859 (2016).
[38] A. Fialkov and A. Loeb, arXiv:1611.01386.
[39] V. F. Baldassare, A. E. Reines, E. Gallo, and J. E. Greene, Astrophys. J. Lett. **809**, L14 (2015).
[40] V. F. Baldassare, A. E. Reines, E. Gallo, and J. E. Greene, Astrophys. J. **836**, 20 (2017).
[41] T. W. S. Holoien *et al.*, Mon. Not. R. Astron. Soc. **455**, 2918 (2016).
[42] M. G. Aartsen *et al.* (IceCube Collaboration), arXiv: 1412.5106.
[43] P. Baerwald, S. Hummer, and W. Winter, Phys. Rev. D **83**, 067303 (2011).
[44] P. Baerwald, S. Hummer, and W. Winter, Astropart. Phys. **35**, 508 (2012).
[45] S. Hummer, P. Baerwald, and W. Winter, Phys. Rev. Lett. **108**, 231101 (2012).
[46] S. Adrian-Martinez *et al.* (ANTARES Collaboration), Astron. Astrophys. **559**, A9 (2013).
[47] A. Mucke, R. Engel, J. Rachen, R. Protheroe, and T. Stanev, Comput. Phys. Commun. **124**, 290 (2000).
[48] S. Hümmer, M. Rüger, F. Spanier, and W. Winter, Astrophys. J. **721**, 630 (2010).
[49] D. Boncioli, A. Fedynitch, and W. Winter, arXiv: 1607.07989.
[50] P. Lipari, M. Lusignoli, and D. Meloni, Phys. Rev. D **75**, 123005 (2007).
[51] T. Kashti and E. Waxman, Phys. Rev. Lett. **95**, 181101 (2005).
[52] B. Chai, X. Cao, and M. Gu, Astrophys. J. **759**, 114 (2012).
[53] A. Tchekhovskoy, R. Narayan, and J. C. McKinney, Mon. Not. R. Astron. Soc. **418**, L79 (2011).
[54] J. C. McKinney, A. Tchekhovskoy, and R. D. Blandford, Mon. Not. R. Astron. Soc. **423**, 3083 (2012).
[55] H. Sun, B. Zhang, and Z. Li, Astrophys. J. **812**, 33 (2015).
[56] C. Patrignani *et al.* (Particle Data Group Collaboration), Chin. Phys. C **40**, 100001 (2016).

[57] S. Ando and K. Sato, New J. Phys. **6**, 170 (2004).
[58] M. G. Aartsen *et al.* (IceCube Collaboration), arXiv: 1510.05223.
[59] M. G. Aartsen *et al.* (IceCube Collaboration), Astrophys. J. **809**, 98 (2015).
[60] P. Baerwald, M. Bustamante, and W. Winter, Astropart. Phys. **62**, 66 (2015).
[61] M. G. Aartsen *et al.* (IceCube Collaboration) Astrophys. J. **833**, 3 (2016).
[62] A. Palladino and F. Vissani, Astrophys. J. **826**, 185 (2016).
[63] A. Palladino, M. Spurio, and F. Vissani, J. Cosmol. Astropart. Phys. 12 (2016) 045.
[64] M. Bustamante, J. F. Beacom, and W. Winter, Phys. Rev. Lett. **115**, 161302 (2015).
[65] D. Biehl, A. Fedynitch, A. Palladino, T. J. Weiler, and W. Winter, J. Cosmol. Astropart. Phys. 01 (2017) 033.
[66] K. Murase, K. Ioka, S. Nagataki, and T. Nakamura, Phys. Rev. D **78**, 023005 (2008).
[67] M. M. Reynoso and G. E. Romero, Astron. Astrophys. **493**, 1 (2009).
[68] L. Dai and K. Fang, arXiv:1612.00011.
[69] N. Senno, K. Murase, and P. Meszaros, Astrophys. J. **838**, 3 (2017).
[70] E. Waxman and J. N. Bahcall, Phys. Rev. Lett. **78**, 2292 (1997).
[71] D. Guetta, D. Hooper, J. Alvarez-Muniz, F. Halzen, and E. Reuveni, Astropart. Phys. **20**, 429 (2004).
[72] Z. Li, Phys. Rev. D **85**, 027301 (2012).
[73] R. S. Warwick and T. P. Roberts, Astron. Nachr. **319**, 59 (1998).
[74] R. Gilli, Adv. Space Res. **34**, 2470 (2004).